Neural Processing Letters (2023) 55:3509–3531
https://doi.org/10.1007/s11063-022-11020-3

Adaptive Decentralized Tracking Control for a Class of Large-Scale Nonlinear Systems with Dynamic Uncertainties Using Multi-dimensional Taylor Network Approach

Zheng-Duo Shan[1] · Wen-Jing He[1] · Yu-Qun Han[1,2] · Shan-Liang Zhu[1,2]

Accepted: 22 August 2022 / Published online: 6 September 2022

Abstract
For the large-scale nonlinear systems subject to dynamic uncertainties, an adaptive multi-dimensional Taylor network (MTN)-based decentralized control strategy is proposed, which can effectively solve output tracking control problem of the systems. Firstly, a dynamic signal is introduced to cope with the problem of unknown nonlinear dynamic uncertainties. Secondly, in each step of the backstepping, only one MTN is used to approximate the combination of unknown nonlinear functions. Then, in the last step of the backstepping, a new adaptive control scheme is designed, which realizes the stability and boundedness of the controlled systems. It is worth noting that the large-scale nonlinear systems, the unknown dynamic uncertainties and the MTN appear in the same framework for the first time. Finally, three simulation examples are presented to verify the feasibility of the proposed control strategy.

Keywords Large-scale nonlinear systems · Dynamic uncertainties · Multi-dimensional Taylor network · Adaptive control

1 Introduction

In recent years, with the development of production and the progress of science and technology, plenty of practical systems can be modeled as large-scale systems have received more and more attention, such as the power systems [1], the transportation network systems [2], the aerospace systems [3] and the manufacturing systems [4]. Therefore, the research on large-scale nonlinear systems turns into a hotspot of society [5–7]. However, due to the characteristics of the large-scale nonlinear systems, such as numerous influencing factors, complex structures, strong randomness and scattered controlled objects, it is very difficult to adopt centralized control. For this reason, the application of decentralized control in large-scale

✉ Shan-Liang Zhu
zhushanliang@qust.edu.cn

1 School of Mathematics and Physics, Qingdao University of Science and Technology, Qingdao 266061, China

2 The Research Institute for Mathematics and Interdisciplinary Sciences, Qingdao University of Science and Technology, Qingdao 266061, China

nonlinear systems is more and more extensive owing to its advantages of strong pertinence and system adaptability [8, 9]. At the same time, adaptive control has been proved to be an effective method to deal with the control issue of uncertain systems containing a large number of stochastic factors [10, 11]. Especially, the design process of control strategy of nonlinear systems can be greatly simplified by combining adaptive control approach with backstepping technique. Therefore, adaptive backstepping control method provides a systematic methodology of solving the control issues of uncertain nonlinear systems, and received a lot of attention [12, 13]. From the above discussed, it is of important practical significance to develop an adaptive backstepping decentralized control strategy for large-scale nonlinear systems [14, 15]. Sad to say, when the system with complex structures and uncertainties, the above control methods may fail to maintain a good performance.

With the aim of solving the above problem, two general approximation methods, fuzzy logic systems (FLSs) and neural networks (NNs) are widely applied in plenty of large-scale systems, such as large-scale nonlinear systems [16, 17], large-scale switched nonlinear systems [18, 19], large-scale stochastic nonlinear systems [20, 21]. In the recent period of time, multi-dimensional Taylor network (MTN), a new type of NN, was verified as an effective and simple method to cope with the control problem of systems with unknown structures, such as nonlinear systems [22], discrete nonlinear systems [23], switched nonlinear systems [24] and stochastic nonlinear systems [25]. Significantly, for large-scale nonlinear systems, many adaptive decentralized backstepping control strategies based on MTN were reported, which demonstrated the practicability of the MTN approximation technique [26, 27]. Unluckily, neither unmodeled dynamics nor dynamic disturbances were considered in the above studies.

In fact, the unmodeled dynamics and dynamic disturbances are inevitably involved in practice [28, 29], their existence is a source of instability of the control systems. Therefore, more and more attention has been devoted to the investigation on systems with dynamic uncertainties. For example, the authors in [30] introduced a dynamic signal to deal with the dynamic uncertainties, which was extended to plenty of nonlinear systems, such as switched nonlinear systems [31], stochastic nonlinear systems [32] and uncertain nonlinear systems [33]. According to the method of introducing a dynamic signal, many adaptive FLS-based decentralized control strategies were put forward for large-scale nonlinear systems with dynamic uncertainties [34, 35]. In spite of these excellent results, it should be pointed out that the adaptive NN-based decentralized control of large-scale nonlinear systems with dynamic uncertainties is still an open issue. Therefore, it is a challenging task to propose a simple and practically feasible adaptive NN-based decentralized control method by introducing a dynamic signal.

Based on the above analysis, the MTN-based tracking control strategy for a class of large-scale nonlinear systems with dynamic uncertainties is developed in this paper. Firstly, the goal of controlling dynamic uncertainties is achieved by introducing a dynamic signal. Secondly, as a novel NN with special structures, MTN technique is employed to estimate the systems parameter and complex unknown nonlinear structures in the design process of backstepping control. Then, an adaptive MTN-based decentralized control strategy is put forward. The simulation results indicate that the control strategy proposed in this paper is satisfactory. In a word, the main contributions of this paper are as follows:

(1) As a new type of NN, MTN opens up a new way for the control issue of large-scale nonlinear systems subject to dynamic uncertainties. Although the author on [36] proposed an adaptive MTN control strategy for nonlinear systems with unmodeled dynamics, this strategy is not suitable to control large-scale nonlinear systems. The adaptive MTN-based decentralized control issues for large-scale nonlinear systems were studied in [26,

27], but the unmodeled dynamics and the dynamic disturbances were not involved in the controlled systems.

(2) Different from the studies in [36–40], the control issue considered in this paper is more general. The result of this paper can be used to deal with large-scale nonlinear systems with dynamic disturbance, which has a wider application scope. By introducing a dynamic signal in the control process, a novel NN-based control method is proposed, which shows the superiority of adaptive MTN-based decentralized control in dynamic uncertainties and complex structures. In addition, although similar control problems were discussed in [34, 35], a MTN-based control approach with simple structure and low computational complexity is developed.

(3) To the authors' knowledge, this paper is the first fruitful work to investigate the MTN-based tracking control of large-scale nonlinear systems with unmodeled dynamics and dynamic disturbances. It is difficult to develop a decentralized control scheme, which can obtain relatively ideal control effect with smaller cost of calculation. Thanks to the simple structure of MTN, the control strategy developed in this paper has the advantages of simple structure and small calculation.

Notation For the matrix or vector $\boldsymbol{x}$, $\boldsymbol{x}^{\mathrm{T}}$ represents its transpose, $|\boldsymbol{x}|$ defines its absolute value. Γ^{-1} indicates the inverse of the given matrix Γ. $\mathbb{R}^i$ denotes i-dimensional real space.

2 System Statements and Preliminaries

2.1 Problem Formulation

A class of large-scale nonlinear systems subject to dynamic uncertainties with N subsystems is considered as follows

$$\begin{cases} \dot{\xi}_i = q_i(\xi_i, \boldsymbol{x}_i) \\ \dot{x}_{i,j} = g_{i,j}\left(\overline{\boldsymbol{x}}_{i,j}\right)x_{i,j+1} + f_{i,j}\left(\overline{\boldsymbol{x}}_{i,j}\right) + h_{i,j}(\boldsymbol{y}) + \Delta_{i,j}(\boldsymbol{x}_i, \xi_i) \\ \dot{x}_{i,n_i} = g_{i,n_i}\left(\overline{\boldsymbol{x}}_{i,n_i}\right)u_i + f_{i,n_i}\left(\overline{\boldsymbol{x}}_{i,n_i}\right) + h_{i,n_i}(\boldsymbol{y}) + \Delta_{i,n_i}\left(\boldsymbol{x}_{n_i}, \xi_{n_i}\right) \\ y_i = x_{i,1} \end{cases}, \tag{1}$$

where $i = 1, \ldots, N$, $j = 1, \ldots, n_i - 1$. $\boldsymbol{x}_i = \left[x_{i,1}, \ldots, x_{i,n_i}\right]^{\mathrm{T}} \in \mathbb{R}^{n_i}$, $u_i \in \mathbb{R}$ and $y_i \in \mathbb{R}$ are the state vector, the control input and the output of the systems, respectively, $\overline{\boldsymbol{x}}_{i,j} = \left[x_{i,1}, \ldots, x_{i,j}\right]^{\mathrm{T}} \in \mathbb{R}^j$, $\overline{\boldsymbol{x}}_{i,n_i} = \left[x_{i,1}, \ldots, x_{i,n_i}\right]^{\mathrm{T}} \in \mathbb{R}^{n_i}$, $\boldsymbol{y} = [y_1, \ldots, y_N]^{\mathrm{T}} \in \mathbb{R}^N$. In addition, the unmeasured portion of the state is denoted as $\xi_i \in \mathbb{R}^{n_{i,0}}$. ξ_i-dynamics in (1) is unmodeled dynamics. $\Delta_{i,j}(\boldsymbol{x}_i, \xi_i)$ denotes the dynamic disturbances. $f_{i,j}(\cdot)$, $h_{i,j}(\cdot)$ and $q_i(\cdot)$ are unknown smooth functions with $f_{i,j}(\mathbf{0}) = 0$. $g_{i,j}(\cdot)$ indicates the control coefficient, which sign is the control direction of i-th channel.

The control objective of this paper is to design an adaptive MTN controller for the systems (1) such that the systems output y_i follows the desired reference signal $y_{i,d}$, and all the signals in the closed-loop systems are semi-globally bounded.

Assumption 1 [41] The desired reference signal $y_{i,d}$ and its time derivatives up to the n_i-th order $y_{i,d}^{(n_i)}$ are bounded and continuous.

Assumption 2 [25] The sign of the function $g_{i,j}\left(\overline{\boldsymbol{x}}_{i,j}\right)$ is determinable. There are two known constants b_m and b_M, such that $0 < b_m < \left|g_{i,j}\left(\overline{\boldsymbol{x}}_{i,j}\right)\right| < b_M < \infty$ holds.

Assumption 3 [39] In large-scale nonlinear systems (1), $q_i(\boldsymbol{x}_i, \xi_i)$ and $\Delta_{i,j}(\boldsymbol{x}_i, \xi_i)$ are uncertain Lipschitz continuous functions.

Assumption 4 [39] For the dynamic disturbance $\Delta_{i,j}(\boldsymbol{x}_i, \xi_i)$, there are two unknown nonnegative increasing smooth functions $\varphi_{i,j}(\cdot)$ and $\psi_{i,j}(\cdot)$ with $\psi_{i,j}(0) = 0$, such that

$$\left|\Delta_{i,j}(\boldsymbol{x}_i, \xi_i)\right| \leq \varphi_{i,j}\left(\left|\boldsymbol{x}_{i,j}\right|\right) + \psi_{i,j}(|\xi_i|). \tag{2}$$

Assumption 5 [30] For $\dot{\xi}_i = q_i(\xi_i, \boldsymbol{x}_i)$, there exist an exponentially input-to-state practically stable Lyapunov function $V_i(\xi_i)$, such that

$$\kappa_{i,1}(|\xi_i|) \leq V_i(\xi_i) \leq \kappa_{i,2}(|\xi_i|), \tag{3}$$

$$\frac{\partial V_i(\xi_i)}{\partial \xi_i} q_i(\xi_i, \boldsymbol{x}_i) \leq -c_{i,0} V_i(\xi_i) + \kappa_{i,3}(|\boldsymbol{x}_i|) + d_{i,0}, \tag{4}$$

where $c_{i,0}, d_{i,0} > 0$ define known constants and $\kappa_{i,1}$, $\kappa_{i,2}$ and $\kappa_{i,3}$ belong to class κ_∞ functions.

Assumption 6 [26] For the unknown smooth function $h_{i,j}(\boldsymbol{y})$, there exists the unknown function $h_{i,j,l}(\cdot)$, such that

$$\left|h_{i,j}(\boldsymbol{y})\right|^2 \leq \sum_{l=1}^{N} h_{i,j,l}^2(y_l), \tag{5}$$

where $h_{i,j,l}(0) = 0, \;\; l = 1, \ldots, N$.

Remark 1 In the light of Assumption 6, there exists the unknown smooth function $\tilde{h}_{i,j,l}(y_l)$, such that

$$\left|h_{i,j}(\boldsymbol{y})\right|^2 \leq \sum_{l=1}^{N} y_l^2 \tilde{h}_{i,j,l}^2(y_l). \tag{6}$$

Next, in order to facilitate the theoretical analysis, several useful lemmas are introduced.

Lemma 1 [30] *Based on Assumption 5, for $\dot{\xi}_i = q_i(\xi_i, \boldsymbol{x}_i)$, there exists a Lyapunov function $V_i(\xi_i)$, which satisfies (3) and (4). Then, for the initial value $\xi_{i,0} = \xi_{i,0}(0)$, there exist a nonnegative function $D_i(t)$ defined for all $t \geq 0$ and a finite time $T_{i,0} = T_{i,0}\left(\overline{c}_i, r_{i,0}, \xi_{i,0}\right)$, one has*

$$V_i(\xi_i(t)) \leq r_i(t) + D_i(t), \tag{7}$$

where $D_i(t) = 0, \forall t \geq T_{i,0}$. r_i is a novel signal, and its time derivative can be expressed as

$$\dot{r}_i = -\overline{c}_i r_i + \overline{\kappa}_{i,3}\left(x_{i,1}\right) + d_{i,0}, \;\; r_i(0) = r_{i,0}, \tag{8}$$

where $r_{i,0}$ is an arbitrary positive constant, and $\overline{c}_i \in \left(0, c_{i,0}\right)$. The function $\overline{\kappa}_{i,3}(\cdot)$ satisfies $\overline{\kappa}_{i,3}\left(x_{i,1}\right) \geq \kappa_{i,3}\left(\left|x_{i,1}\right|\right)$.

Remark 2 If $\overline{\kappa}_{i,3}(\cdot)$ satisfies $\overline{\kappa}_{i,3}(s) = \left(s - y_{i,d}\right)^2 \kappa_i\left(s^2\right)$, Then, (8) can be described as

$$\dot{r}_i = -\overline{c}_i r_i + \left(x_{i,1} - y_{i,d}\right)^2 \kappa_i\left(\left|x_{i,1}\right|^2\right) + d_{i,0}, \;\; r_i(0) = r_{i,0}, \tag{9}$$

where $\kappa_i(\cdot)$ is a nonnegative smooth function. $\overline{\kappa}_{i,3}(\cdot)$ is a smooth function, which satisfies $\overline{\kappa}_{i,3}(0) \geq 0$.

Remark 3 Different from [40], a novel function $\overline{\kappa}_{i,3}(\cdot)$ is introduced. In addition, for the issue of stabilization of large-scale nonlinear systems, we consider that $\overline{\kappa}_{i,3}$ satisfies $\overline{\kappa}_{i,3}(s) = s^2\kappa_i\left(s^2\right)$.

Lemma 2 [39] *For any nonnegative constant* ε *and any value* $x \in \mathbb{R}$, *there exists a smooth function* $Q(\cdot) : \mathbb{R} \to \mathbb{R}$, *such that*

$$|x| \le xQ(x) + \varepsilon, \tag{10}$$

where $Q(0) = 0$.

Lemma 3 [39] *For a nonnegative constant* ε *and any continuous function* $P(\cdot) : \mathbb{R} \to \mathbb{R}$, *there exists a nonnegative smooth function* $\hat{P}(\cdot)$, *such that*

$$|P(x)| \le \hat{P}(x) + \varepsilon, \forall x \in \mathbb{R}, \tag{11}$$

where $P(\cdot)$ *satisfies* $P(0) = 0$, $\hat{P}(\cdot)$ *satisfies* $\hat{P}(0) = 0$ *and* $\left.\frac{\partial \hat{P}}{\partial x}\right|_{x=0} = 0$.

2.2 Multi-dimensional Taylor Network

In this paper, for $\forall\varsigma > 0$, an unknown smooth nonlinear function $f(\boldsymbol{\Lambda})$ on a compact set $\Omega_{\boldsymbol{\Lambda}}$ can be approximated by the following MTN.

$$f(\boldsymbol{\Lambda}) = \boldsymbol{\theta}^{*\mathrm{T}} S_{m_n}(\boldsymbol{\Lambda}) + \sigma(\boldsymbol{\Lambda}), \tag{12}$$

with the optimal weight vector $\boldsymbol{\theta}^*$ is defines as

$$\boldsymbol{\theta}^* := \arg\min_{\boldsymbol{\theta}\in\mathbb{R}^l}\left\{\sup_{\boldsymbol{\Lambda}\in\Omega_{\boldsymbol{\Lambda}}}\left|f(\boldsymbol{\Lambda}) - \boldsymbol{\theta}^{\mathrm{T}} S_{m_n}(\boldsymbol{\Lambda})\right|\right\}, \tag{13}$$

where $\boldsymbol{\theta} = [\theta_1, \ldots, \theta_l]^{\mathrm{T}}$ is the weight vector of MTN. $\boldsymbol{\Lambda} = [\Lambda_1, \ldots, \Lambda_n]^{\mathrm{T}}$ are the input vector. $S_{m_n}(\boldsymbol{\Lambda}) = \left[\Lambda_1, \ldots, \Lambda_n, \Lambda_1^2, \ldots, \Lambda_n^2, \ldots, \Lambda_1^m, \ldots, \Lambda_n^m\right]^{\mathrm{T}} \subset \mathbb{R}^l$ is the middle layer vector. l, n are the number of middle layer and input dimensions of MTN, respectively. $\sigma(\boldsymbol{\Lambda})$ denotes the MTN inherent approximation error and $|\sigma(\boldsymbol{\Lambda})| < \varsigma$. MTN is a feedforward network with n inputs and m highest power, and its structure is shown in Fig. 1.

3 Main Results

3.1 Recursive Design of Adaptive Controller

Step i, 1: For $i = 1, \ldots, N$, $j = 1, \ldots, n_i - 1$, a coordinate transformation is defined as

$$\begin{cases} z_{i,1} = x_{i,1} - y_{i,d} \\ z_{i,j+1} = x_{i,j+1} - \alpha_{i,j} \end{cases}, \tag{14}$$

with $\alpha_{i,j}$ is the virtual control signal.

The candidate Lapunov function is selected as

$$V_{i,1} = \frac{1}{2}z_{i,1}^2 + \frac{1}{\lambda_{i,0}}r_i + \frac{1}{2}\tilde{\boldsymbol{\theta}}_{i,1}^{\mathrm{T}}\Gamma_{i,1}^{-1}\tilde{\boldsymbol{\theta}}_{i,1}, \tag{15}$$

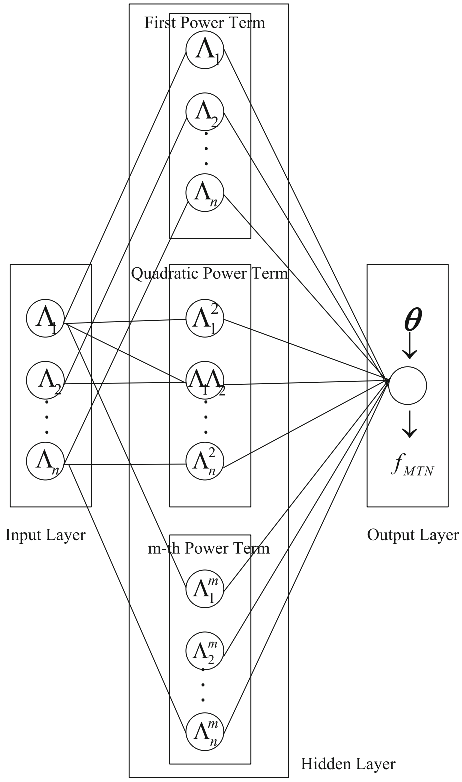

Fig. 1 Network structure of MTN

where $\tilde{\boldsymbol{\theta}}_{i,1} = \boldsymbol{\theta}_{i,1} - \hat{\boldsymbol{\theta}}_{i,1}$ is the parameter error, $\hat{\boldsymbol{\theta}}_{i,1}$ denotes the estimated value of $\boldsymbol{\theta}_{i,1}$. $\Gamma_{i,1} = \Gamma_{i,1}^{\mathrm{T}} > 0$ is an arbitrary constant matrix. $\lambda_{i,0}$ is a positive design parameter.

The time derivative of $V_{i,1}$ can be obtained as follows

$$\dot{V}_{i,1} = z_{i,1}\dot{z}_{i,1} + \frac{1}{\lambda_{i,0}}\dot{r}_i - \tilde{\boldsymbol{\theta}}_{i,1}^{\mathrm{T}}\Gamma_{i,1}^{-1}\dot{\hat{\boldsymbol{\theta}}}_{i,1}. \tag{16}$$

According to (1), (9), (14), Assumption 4 and Lemma 1, the following inequality can be obtained

$$\begin{aligned}\dot{V}_{i,1} \le{} & z_{i,1}\left(g_{i,1}x_{i,2} + f_{i,1} + h_{i,1} - \dot{y}_{i,d}\right) + \left|z_{i,1}\right|\varphi_{i,1}\left(\left|\overline{x}_{i,1}\right|\right) + \left|z_{i,1}\right|\psi_{i,1}(|\xi_i|)\\ & + \frac{1}{\lambda_{i,0}}\left(z_{i,1}^2\kappa_i\left(\left|x_{i,1}\right|^2\right) + d_{i,0}\right) - \frac{1}{\lambda_{i,0}}\overline{c}_i r_i - \tilde{\boldsymbol{\theta}}_{i,1}^{\mathrm{T}}\Gamma_{i,1}^{-1}\dot{\hat{\boldsymbol{\theta}}}_{i,1}.\end{aligned} \tag{17}$$

According to Lemmas 2 and 3, the following inequality holds

$$\left|z_{i,1}\right|\varphi_{i,1}\left(\left|\overline{x}_{i,1}\right|\right) \le z_{i,1}\tilde{\varphi}_{i,1}\left(\overline{x}_{i,1}\right) + \varepsilon_{i,1}, \tag{18}$$

with $\varepsilon_{i,1} > 0$ is a constant.

According to [30], there exists a smooth function $\hat{\psi}_{i,1,2}(\cdot)$ with $\hat{\psi}_{i,1,2}(0) = 0$, such that

$$\left|z_{i,1}\right|\psi_{i,1}(|\xi_i|) \le z_{i,1}\tilde{\psi}_{i,1}\left(z_{i,1}, r_i\right) + 2\delta_{i,1} + \frac{1}{4}z_{i,1}^2 + d_{i,1}(t), \tag{19}$$

where $\tilde{\psi}_{i,1}(z_{i,1}, r_i) = \hat{\psi}_{i,1,2}(r_i)\hat{\psi}_{i,1,3}(z_{i,1}, r_i) + \hat{\psi}_{i,1,4}(z_{i,1})$, $d_{i,1}(t) = \big(\psi_{i,1,2}\circ \kappa_{i,1}^{-1}(2D_i(t))\big)$ and $d_{i,1}(t) = 0$, $\forall t \geq T_{i,0}$. $\hat{\psi}_{i,1,3}$, $\hat{\psi}_{i,1,4}$ are two suitable smooth functions with $\hat{\varphi}_{i,1,3}(0) = 0$, $\hat{\varphi}_{i,1,4}(0) = 0$. $\delta_{i,1} > 0$ is a constant.

According to Young's inequality and Assumption 6, the following inequality can be obtained

$$z_{i,1}h_{i,1} \leq \frac{1}{2}z_{i,1}^2 + \frac{1}{2}h_{i,1}^2 \leq \frac{1}{2}z_{i,1}^2 + \frac{1}{2}\sum_{l=1}^{N} y_l^2\tilde{h}_{i,1,l}^2(y_l). \tag{20}$$

Substituting (18), (19) and (20) into (17), the following inequality holds

$$\begin{aligned}\dot{V}_{i,1} \leq\ & z_{i,1}\Big(g_{i,1}x_{i,2} + \tilde{f}_{i,1}\Big) - \upsilon_{i,1}^2\big(z_{i,1}^2\big)z_{i,1}^2 - \frac{1}{2}z_{i,1}^2 + \frac{1}{2}\sum_{l=1}^{N} y_l^2\tilde{h}_{i,1,l}^2(y_l)\\ &+ \varepsilon_{i,1} + 2\delta_{i,1} + d_{i,1}(t) + \frac{1}{\lambda_{i,0}}d_{i,0} - \frac{1}{\lambda_{i,0}}\bar{c}_i r_i - \tilde{\boldsymbol{\theta}}_{i,1}^{\mathrm{T}}\Gamma_{i,1}^{-1}\dot{\hat{\boldsymbol{\theta}}}_{i,1},\end{aligned} \tag{21}$$

where $\tilde{f}_{i,1} = f_{i,1} - \dot{y}_{i,d} + \tilde{\varphi}_{i,1}(\overline{x}_{i,1}) + \tilde{\psi}_{i,1}(z_{i,1}, r_i) + \frac{5}{4}z_{i,1} + \frac{1}{\lambda_{i,0}}z_{i,1}\kappa_i\Big(\big|x_{i,1}\big|^2\Big) + \upsilon_{i,1}^2\Big(z_{i,1}^2\Big)z_{i,1}$.

$\tilde{f}_{i,1}$ is a combination of unknown nonlinear functions, which cannot be used to construct the virtual control signal $\alpha_{i,1}$. According to the approximation performance of MTN, for any given constant $\varsigma_{i,1} > 0$, there exists a MTN $\boldsymbol{\theta}_{i,1}^{\mathrm{T}}S_{m_{i,1}}$, such that

$$\tilde{f}_{i,1} = \boldsymbol{\theta}_{i,1}^{\mathrm{T}}S_{m_{i,1}} + \sigma_{i,1}, \quad \big|\sigma_{i,1}\big| \leq \varsigma_{i,1}, \tag{22}$$

where $\sigma_{i,1}$ is the estimate error.

According to (22) and Young's inequality, the following inequality holds

$$z_{i,1}\tilde{f}_{i,1} = z_{i,1}\boldsymbol{\theta}_{i,1}^{\mathrm{T}}S_{m_{i,1}} + z_{i,1}\sigma_{i,1} \leq z_{i,1}\boldsymbol{\theta}_{i,1}^{\mathrm{T}}S_{m_{i,1}} + \frac{1}{2}z_{i,1}^2 + \frac{1}{2}\varsigma_{i,1}^2. \tag{23}$$

With the help of (14), (21) and (23), the following inequality can be obtained

$$\begin{aligned}\dot{V}_{i,1} \leq\ & g_{i,1}z_{i,1}\big(z_{i,2} + \alpha_{i,1}\big) + z_{i,1}\boldsymbol{\theta}_{i,1}^{\mathrm{T}}S_{m_{i,1}} - \upsilon_{i,1}^2\big(z_{i,1}^2\big)z_{i,1}^2 + \frac{1}{2}\sum_{l=1}^{N} y_l^2\tilde{h}_{i,1,l}^2(y_l)\\ &+\frac{1}{2}\varsigma_{i,1}^2 + \varepsilon_{i,1} + 2\delta_{i,1} + d_{i,1}(t) + \frac{1}{\lambda_{i,0}}d_{i,0} - \frac{1}{\lambda_{i,0}}\bar{c}_i r_i - \tilde{\boldsymbol{\theta}}_{i,1}^{\mathrm{T}}\Gamma_{i,1}^{-1}\dot{\hat{\boldsymbol{\theta}}}_{i,1},\end{aligned} \tag{24}$$

According to Young's inequality, one has

$$g_{i,1}z_{i,1}z_{i,2} \leq \frac{1}{2}g_{i,1}z_{i,1}^2 + \frac{1}{2}g_{i,1}z_{i,2}^2. \tag{25}$$

Choosing the virtual control signal $\alpha_{i,1}$ as follows

$$\alpha_{i,1} = -\frac{1}{b_m}\Big(r_{i,1}z_{i,1}+\hat{\boldsymbol{\theta}}_{i,1}^{\mathrm{T}}S_{m_{i,1}}\Big), \tag{26}$$

where $r_{i,1} > 0$ is a constant.

According to Assumption 2, the following inequality can be obtained.

$$g_{i,1}z_{i,1}\alpha_{i,1} = -\frac{1}{b_m}g_{i,1}z_{i,1}\Big(r_{i,1}z_{i,1}+\hat{\boldsymbol{\theta}}_{i,1}^{\mathrm{T}}S_{m_{i,1}}\Big) \leq -r_{i,1}z_{i,1}^2 - z_{i,1}\hat{\boldsymbol{\theta}}_{i,1}^{\mathrm{T}}S_{m_{i,1}}. \tag{27}$$

Substituting (25) and (27) into (24), the following inequality holds

$$\dot{V}_{i,1} \leq -\left(r_{i,1} - \frac{1}{2}g_{i,1}\right)z_{i,1}^2 + \frac{1}{2}g_{i,1}z_{i,2}^2 - \upsilon_{i,1}^2\left(z_{i,1}^2\right)z_{i,1}^2 + \frac{1}{2}\sum_{l=1}^{N} y_l^2 \tilde{h}_{i,1,l}^2(y_l)$$
$$+ \frac{1}{2}\varsigma_{i,1}^2 + \varepsilon_{i,1} + 2\delta_{i,1} + d_{i,1}(t) + \frac{1}{\lambda_{i,0}}d_{i,0} - \frac{1}{\lambda_{i,0}}\bar{c}_i r_i + \tilde{\boldsymbol{\theta}}_{i,1}^{\mathrm{T}}\left(z_{i,1}S_{m_{i,1}} - \Gamma_{i,1}^{-1}\dot{\hat{\boldsymbol{\theta}}}_{i,1}\right). \tag{28}$$

Step i, k $(2 \leq k \leq n_i - 1)$: For the systems (1), after a series of mathematical derivations, a result similar to (28) can be obtained. It can be summarized as the following lemma.

Lemma 4 *For* $k = 1, 2, \ldots, n_i - 1$, *the candidate Lapunov function is selected as* $V_{i,k} = V_{i,k-1} + \frac{1}{2}z_{i,k}^2 + \frac{1}{2}\tilde{\boldsymbol{\theta}}_{i,k}^{\mathrm{T}}\Gamma_{i,k}^{-1}\tilde{\boldsymbol{\theta}}_{i,k}$, *the following inequality can be obtained*

$$\dot{V}_{i,k} \leq -\sum_{j=1}^{k}\left(r_{i,j} - \frac{1}{2}g_{i,j}\right)z_{i,j}^2 + \frac{1}{2}\sum_{j=1}^{k} g_{i,j}z_{i,j+1}^2 - \upsilon_{i,1}^2\left(z_{i,1}^2\right)z_{i,1}^2 + \frac{1}{2}\sum_{j=1}^{k}\sum_{l=1}^{N} y_l^2 \tilde{h}_{i,j,l}^2(y_l)$$
$$+ \frac{1}{2}\sum_{j=1}^{k}\varsigma_{i,j}^2 + \sum_{j=1}^{k}\varepsilon_{i,j} + 2\sum_{j=1}^{k} j\delta_{i,j} + \sum_{j=1}^{k} d_{i,j}(t) + \frac{1}{\lambda_{i,0}}d_{i,0} - \frac{1}{\lambda_{i,0}}\bar{c}_i r_i$$
$$+ \sum_{j=1}^{k}\tilde{\boldsymbol{\theta}}_{i,j}^{\mathrm{T}}\left(z_{i,j}S_{m_{i,j}} - \Gamma_{i,j}^{-1}\dot{\hat{\boldsymbol{\theta}}}_{i,j}\right). \tag{29}$$

where $r_{i,j}, \varsigma_{i,j}, \varepsilon_{i,j}, \delta_{i,j}$ *are positive design constants,* $\tilde{\boldsymbol{\theta}}_{i,j} = \boldsymbol{\theta}_{i,j} - \hat{\boldsymbol{\theta}}_{i,j}$ *defines the parameter error,* $\hat{\boldsymbol{\theta}}_{i,j}$ *denotes the estimated value of* $\boldsymbol{\theta}_{i,j}$, $\Gamma_{i,j} = \Gamma_{i,j}^{\mathrm{T}} > 0$ *is a constant matrix.*

Proof Similar to Step i, 1, according to the recurrence method, Lemma 4 is holds.

Step i, n_i: According to (1) and (14), one has

$$\dot{z}_{i,n_i} = g_{i,n_i}u_i + f_{i,n_i} + h_{i,n_i} + \Delta_{i,n_i} - \dot{\alpha}_{i,n_i-1}, \tag{30}$$

with

$$\dot{\alpha}_{i,n_i-1} = \sum_{j=1}^{n_i-1}\frac{\partial\alpha_{i,n_i-1}}{\partial x_{i,j}}\left(g_{i,j}x_{i,j+1} + f_{i,j} + h_{i,j} + \Delta_{i,j}\right) + \sum_{j=1}^{n_i-1}\frac{\partial\alpha_{i,n_i-1}}{\partial\hat{\boldsymbol{\theta}}_{i,j}}\dot{\hat{\boldsymbol{\theta}}}_{i,j} + \frac{\partial\alpha_{i,n_i-1}}{\partial r_i}\dot{r}_i$$
$$+ \sum_{j=0}^{n_i-1}\frac{\partial\alpha_{i,n_i-1}}{\partial y_{i,d}^{(j)}}y_{i,d}^{(j+1)}.$$

Choosing the candidate Lyapunov function as follows

$$V_{i,n_i} = V_{i,n_i-1} + \frac{1}{2}z_{i,n_i}^2 + \frac{1}{2}\tilde{\boldsymbol{\theta}}_{i,n_i}^{\mathrm{T}}\Gamma_{i,n_i}^{-1}\tilde{\boldsymbol{\theta}}_{i,n_i}, \tag{31}$$

where $\tilde{\boldsymbol{\theta}}_{i,n_i} = \boldsymbol{\theta}_{i,n_i} - \hat{\boldsymbol{\theta}}_{i,n_i}$ is the parameter error, $\hat{\boldsymbol{\theta}}_{i,n_i}$ denotes the estimated value of $\boldsymbol{\theta}_{i,n_i}$, $\Gamma_{i,n_i} = \Gamma_{i,n_i}^{\mathrm{T}} > 0$ is an arbitrary constant matrix.

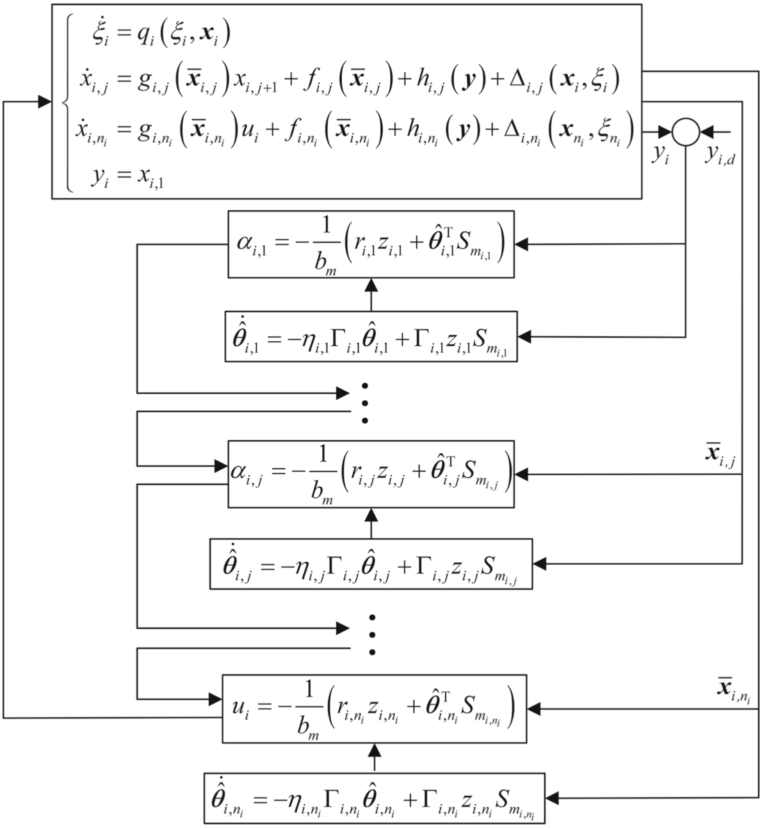

Fig. 2 The design process of the adaptive decentralized MTN-based controller

Then, the time derivative of V_{i,n_i} is as follows

$$\begin{aligned}\dot{V}_{i,n_i} &\le \dot{V}_{i,n_i-1} + z_{i,n_i}\left(g_{i,n_i}u_i + f_{i,n_i} + h_{i,n_i} + \Delta_{i,n_i} - \dot{\alpha}_{i,n_i-1}\right) - \tilde{\boldsymbol{\theta}}_{i,n_i}^{\mathrm{T}}\Gamma_{i,n_i}^{-1}\dot{\hat{\boldsymbol{\theta}}}_{i,n_i} \\ &= \dot{V}_{i,n_i-1} + z_{i,n_i}\left(g_{i,n_i}u_i + f_{i,n_i} + h_{i,n_i} + \overline{\Delta}_{i,n_i} - \sum_{j=1}^{n_i-1}\frac{\partial\alpha_{i,n_i-1}}{\partial x_{i,j}}\left(g_{i,j}x_{i,j+1} + f_{i,j} + h_{i,j}\right)\right. \\ &\quad \left. - \sum_{j=1}^{n_i-1}\frac{\partial\alpha_{i,n_i-1}}{\partial\hat{\boldsymbol{\theta}}_{i,j}}\dot{\hat{\boldsymbol{\theta}}}_{i,j} - \sum_{j=0}^{n_i-1}\frac{\partial\alpha_{i,n_i-1}}{\partial y_{i,d}^{(j)}}y_{i,d}^{(j+1)} - \frac{\partial\alpha_{i,n_i-1}}{\partial r_i}\dot{r}_i\right) - \tilde{\boldsymbol{\theta}}_{i,n_i}^{\mathrm{T}}\Gamma_{i,n_i}^{-1}\dot{\hat{\boldsymbol{\theta}}}_{i,n_i}. \end{aligned} \tag{32}$$

where $\overline{\Delta}_{i,n_i} = \Delta_{i,n_i} - \sum_{j=1}^{n_i-1}\frac{\partial\alpha_{i,n_i-1}}{\partial x_{i,j}}\Delta_{i,j}$.

According to Assumption 4, Lemmas 2 and 3, the following inequalities hold

$$\left|z_{i,n_i}\overline{\Delta}_{i,n_i}\right| \le \left|z_{i,n_i}\right|\left(\varphi_{i,n_i}\left(\left|\overline{\boldsymbol{x}}_{i,n_i}\right|\right) + \sum_{j=1}^{n_i-1}\left|\frac{\partial\alpha_{i,n_i-1}}{\partial x_{i,j}}\right|\varphi_{i,j}\left(\left|\overline{\boldsymbol{x}}_{i,j}\right|\right)\right)$$

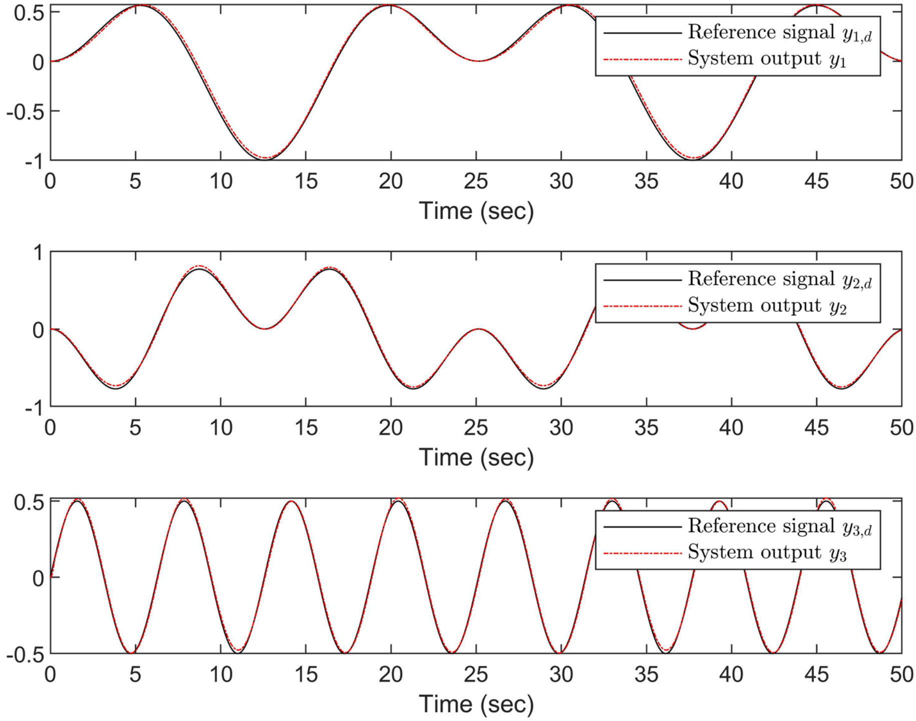

Fig. 3 System output y_i and reference signal $y_{i,d}$ of Example 1

$$+\left|z_{i,n_i}\right|\left(\psi_{i,n_i}(|\xi_i|)+\sum_{j=1}^{n_i-1}\left|\frac{\partial\alpha_{i,n_i-1}}{\partial x_{i,j}}\right|\psi_{i,j}(|\xi_i|)\right), \tag{33}$$

$$\left|z_{i,n_i}\right|\left(\varphi_{i,n_i}\left(\left|\overline{\boldsymbol{x}}_{i,n_i}\right|\right)+\sum_{j=1}^{n_i-1}\left|\frac{\partial\alpha_{i,n_i-1}}{\partial x_{i,j}}\right|\varphi_{i,j}\left(\left|\overline{\boldsymbol{x}}_{i,j}\right|\right)\right)\leq z_{i,n_i}\tilde{\varphi}_{i,n_i}+\varepsilon_{i,n_i}, \tag{34}$$

$$\left|z_{i,n_i}\right|\left(\psi_{i,n_i}(|\xi_i|)+\sum_{j=1}^{n_i-1}\left|\frac{\partial\alpha_{i,n_i-1}}{\partial x_{i,j}}\right|\psi_{i,j}(|\xi_i|)\right)$$
$$\leq z_{i,n_i}\tilde{\psi}_{i,n_i}+\frac{1}{4}z_{i,n_i}^2\left(1+\sum_{j=1}^{n_i-1}\left(\frac{\partial\alpha_{i,n_i-1}}{\partial x_{i,j}}\right)^2\right)+2n_i\delta_{i,n_i}+d_{i,n_i}(t), \tag{35}$$

with $d_{i,n_i}(t)=\sum_{j=1}^{n_i}\left(\psi_{i,j,2}\circ\kappa_{i,1}^{-1}(2D_i(t))\right)^2$ and $d_{i,n_i}(t)=0,\ \forall t\geq T_{i,0}$. $\varepsilon_{i,n_i},\delta_{i,n_i}>0$ are design constants.

According to Assumption 6 and Young's inequality, the following inequality can be obtained

$$z_{i,n_i}h_{i,n_i}\leq\frac{1}{2}z_{i,n_i}^2+\frac{1}{2}h_{i,n_i}^2\leq\frac{1}{2}z_{i,n_i}^2+\frac{1}{2}\sum_{l=1}^{N}y_l^2\tilde{h}_{i,n_i,l}^2(y_l). \tag{36}$$

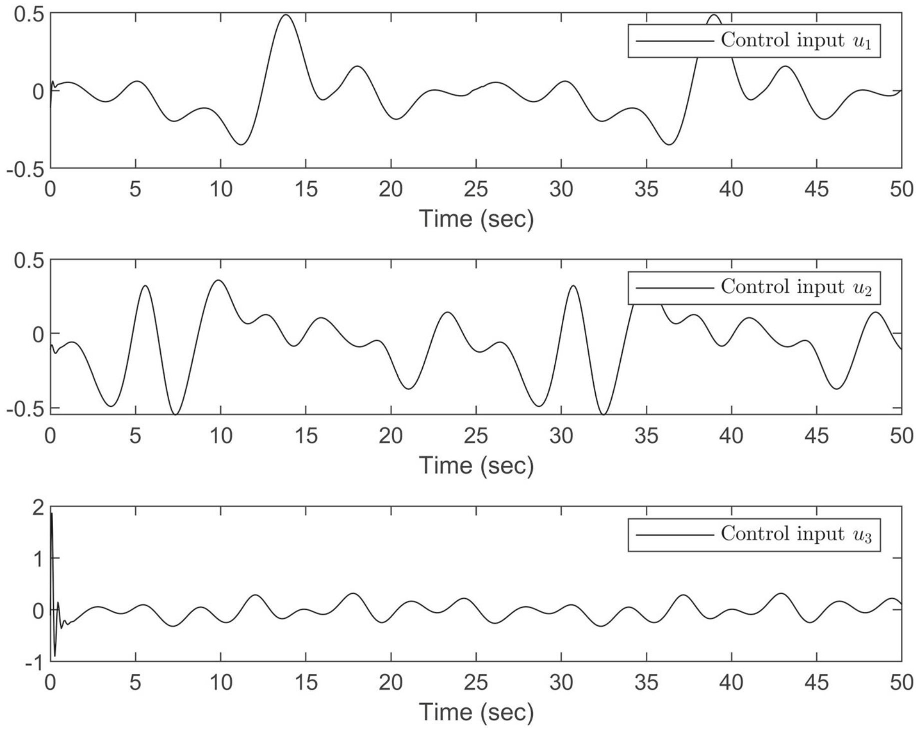

Fig. 4 Control input u_i of Example 1

Combining (32), (33), (34), (35) with (36), the following inequality holds

$$\dot{V}_{i,n_i} \leq \dot{V}_{i,n_i-1} + z_{i,n_i}\left(g_{i,n_i}u_i + \tilde{f}_{i,n_i}\right) - \tilde{\boldsymbol{\theta}}_{i,n_i}^{\mathrm{T}}\Gamma_{i,n_i}^{-1}\dot{\hat{\boldsymbol{\theta}}}_{i,n_i} + \varepsilon_{i,n_i} + 2n_i\delta_{i,n_i} + d_{i,n_i}(t) + \frac{1}{2}\sum_{l=1}^{N} y_l^2\tilde{h}_{i,n_i,l}^2(y_l), \tag{37}$$

where

$$\tilde{f}_{i,n_i} = f_{i,n_i} + \tilde{\varphi}_{i,n_i} + \tilde{\psi}_{i,n_i} + \frac{1}{4}z_{i,n_i}\left(1 + \sum_{j=1}^{n_i-1}\left(\frac{\partial\alpha_{i,n_i-1}}{\partial x_{i,j}}\right)^2\right) + \frac{1}{2}z_{i,n_i} - \frac{\partial\alpha_{i,n_i-1}}{\partial r_i}\dot{r}_i - \sum_{j=1}^{n_i-1}\frac{\partial\alpha_{i,n_i-1}}{\partial x_{i,j}}\left(g_{i,j}x_{i,j+1} + f_{i,j} + h_{i,j}\right) - \sum_{j=1}^{n_i-1}\frac{\partial\alpha_{i,n_i-1}}{\partial\hat{\boldsymbol{\theta}}_{i,j}}\dot{\hat{\boldsymbol{\theta}}}_{i,j} - \sum_{j=0}^{n_i-1}\frac{\partial\alpha_{i,n_i-1}}{\partial y_{i,d}^{(j)}}y_{i,d}^{(j+1)}.$$

$\tilde{f}_{i,n_i}$ is a combination of unknown nonlinear functions, which cannot be used to construct the actual control input signal u_i. According to the approximation performance of MTN, for any given constant $\varsigma_{i,n_i} > 0$, there exists a MTN $\boldsymbol{\theta}_{i,n_i}^{\mathrm{T}}S_{m_{i,n_i}}$, such that

$$\tilde{f}_{i,n_i} = \boldsymbol{\theta}_{i,n_i}^{\mathrm{T}}S_{m_{i,n_i}} + \sigma_{i,n_i},\ \left|\sigma_{i,n_i}\right| \leq \varsigma_{i,n_i}, \tag{38}$$

where σ_{i,n_i} is the estimate error.

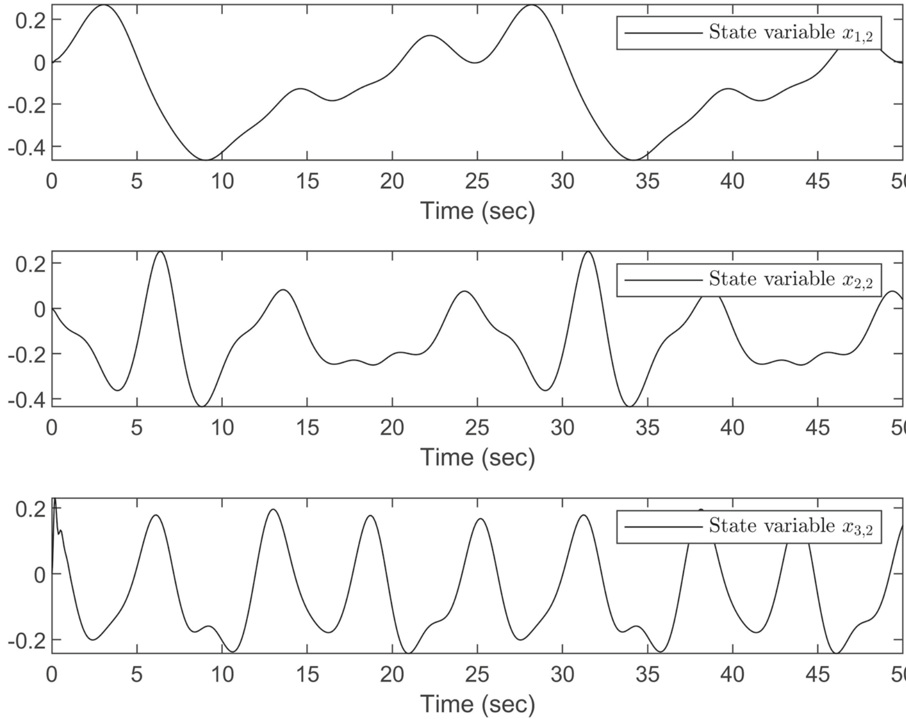

Fig. 5 State variables $x_{i,2}$ of Example 1

According to (38) and Young's inequality, one has

$$z_{i,n_i}\tilde{f}_{i,n_i} \leq z_{i,n_i}\boldsymbol{\theta}_{i,n_i}^{\mathrm{T}}S_{m_{i,n_i}} + \frac{1}{2}z_{i,n_i}^2 + \frac{1}{2}\varsigma_{i,n_i}^2. \tag{39}$$

Choosing the actual control input u_i as follows

$$u_i = -\frac{1}{b_m}\Big(r_{i,n_i}z_{i,n_i} + \hat{\boldsymbol{\theta}}_{i,n_i}^{\mathrm{T}}S_{m_{i,n_i}}\Big), \tag{40}$$

where $r_{i,n_i} > 0$ is a design constant.

By means of combining Assumption 2 and (40), the following inequality holds

$$\begin{aligned} g_{i,n_i}z_{i,n_i}u_i &= -\frac{1}{b_m}g_{i,n_i}z_{i,n_i}\Big(r_{i,n_i}z_{i,n_i} + \hat{\boldsymbol{\theta}}_{i,n_i}^{\mathrm{T}}S_{m_{i,n_i}}\Big) \\ &\leq -r_{i,n_i}z_{i,n_i}^2 - z_{i,n_i}\hat{\boldsymbol{\theta}}_{i,n_i}^{\mathrm{T}}S_{m_{i,n_i}}. \end{aligned} \tag{41}$$

According to Lemma 4 and substituting (39) and (41) into (37), the following inequality can be obtained

$$\begin{aligned} \dot{V}_{i,n_i} \leq &-\sum_{j=1}^{n_i}(r_{i,j} - b_M)z_{i,j}^2 - \upsilon_{i,1}^2(z_{i,1}^2)z_{i,1}^2 + \frac{1}{2}\sum_{j=1}^{n_i}\sum_{l=1}^{N}y_l^2\tilde{h}_{i,j,l}^2(y_l) \\ &+ \frac{1}{2}\sum_{j=1}^{n_i}\varsigma_{i,j}^2 + \sum_{j=1}^{n_i}\varepsilon_{i,j} + 2\sum_{j=1}^{n_i}j\delta_{i,j} + \sum_{j=1}^{n_i}d_{i,j}(t) + \frac{1}{\lambda_{i,0}}d_{i,0} - \frac{1}{\lambda_{i,0}}\bar{c}_i r_i \end{aligned}$$

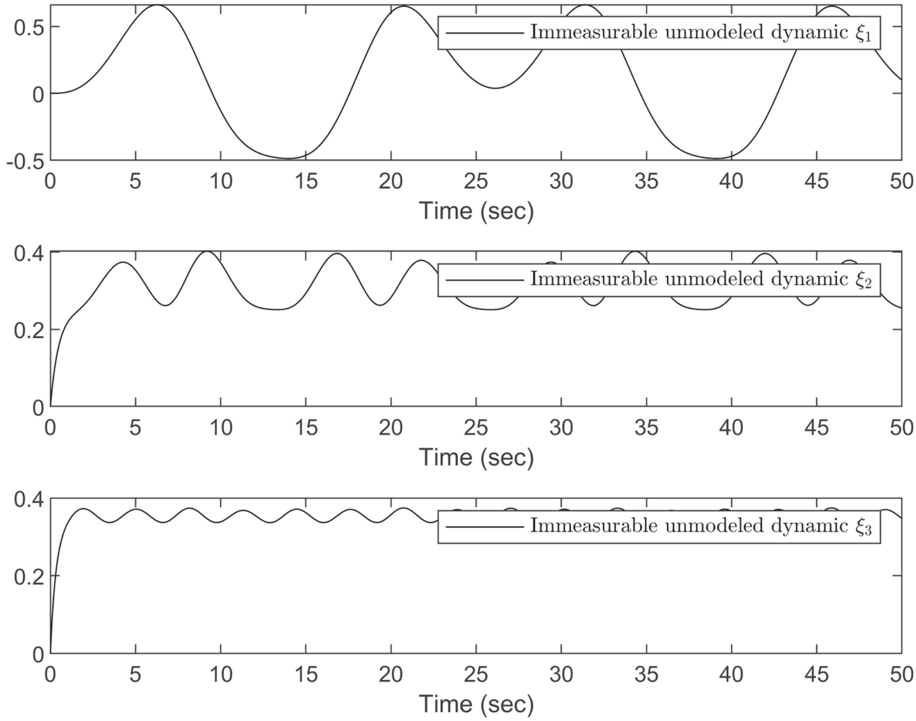

Fig. 6 Immeasurable unmodeled dynamics ξ_i of Example 1

$$+\sum_{j=1}^{n_i}\tilde{\boldsymbol{\theta}}_{i,j}^{\mathrm{T}}\left(z_{i,j}S_{m_{i,j}}-\Gamma_{i,j}^{-1}\dot{\hat{\boldsymbol{\theta}}}_{i,j}\right). \tag{42}$$

Remark 4 Significantly, this paper appears to be the first work dedicated to the MTN-based control of large-scale nonlinear systems with dynamic uncertainties. Compared with [34, 35], the unknown control direction is fully considered, and the controller structure proposed in this paper is relatively simple. Therefore, the proposed MTN-based control strategy has a wider application scope.

3.2 Stability Analysis

Theorem 1 *Considering the large-scale nonlinear systems with dynamic uncertainties, if for* $i=1,\ldots,N$, *actual control input is selected as* (40), *and the virtual control signal is designed as*

$$\alpha_{i,j}=-\frac{1}{b_m}\left(r_{i,j}z_{i,j}+\hat{\boldsymbol{\theta}}_{i,j}^{\mathrm{T}}S_{m_{i,j}}\right),\ \ j=1,\ldots,n_i-1. \tag{43}$$

The adaptive law is constructed as

$$\dot{\hat{\boldsymbol{\theta}}}_{i,j}=-\eta_{i,j}\Gamma_{i,j}\hat{\boldsymbol{\theta}}_{i,j}+\Gamma_{i,j}z_{i,j}S_{m_{i,j}},\ j=1,\ldots,n_i, \tag{44}$$

with $\eta_{i,j}>0$ *is a design constant.*

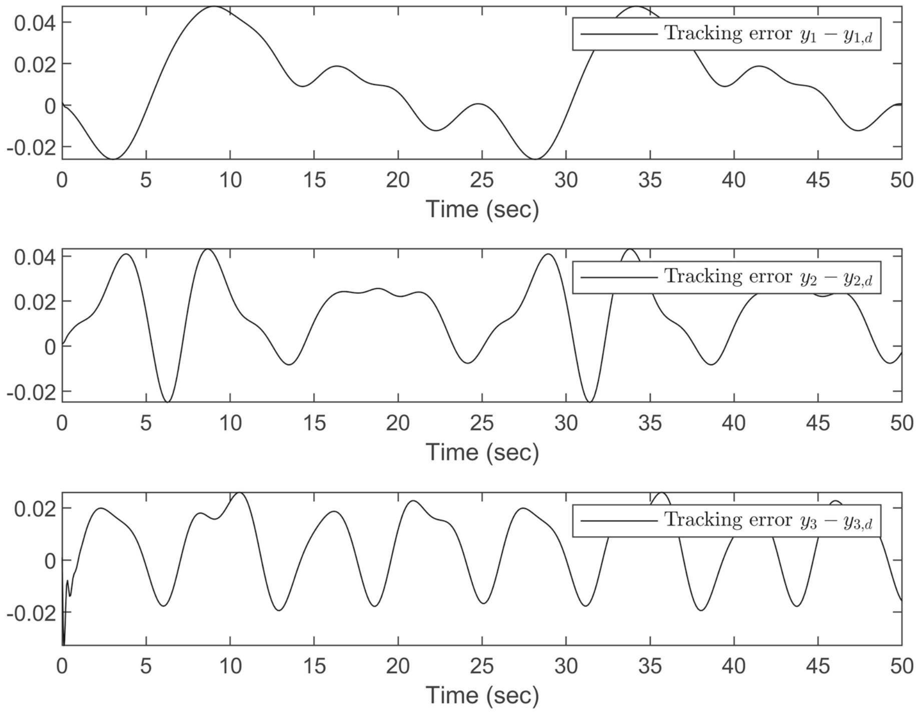

Fig. 7 Tracking error $y_i - y_{i,d}$ of Example 1

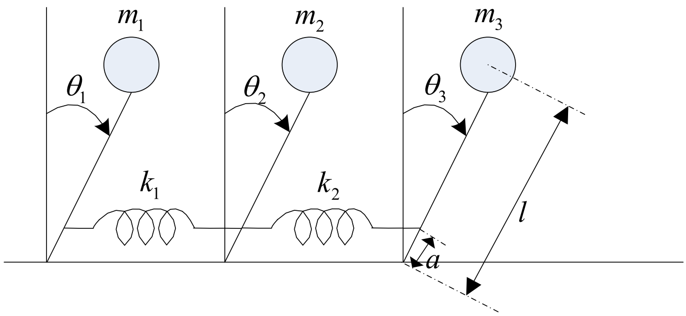

Fig. 8 Schematic of tripled inverted pendulums

Then, for bounded initial conditions, all signals in the closed-loop systems are semi-globally bounded and the tracking error can converge to an adjustable neighborhood of the origin.

Proof Choosing the Lyapunov function as follows

$$V = \frac{1}{2}\sum_{i=1}^{N}\sum_{j=1}^{n_i} z_{i,j}^2 + \frac{1}{2}\sum_{i=1}^{N}\sum_{j=1}^{n_i} \tilde{\boldsymbol{\theta}}_{i,j}^{\mathrm{T}} \Gamma_{i,j}^{-1} \tilde{\boldsymbol{\theta}}_{i,j} + \sum_{i=1}^{N} \frac{1}{\lambda_{i,0}} r_i. \tag{45}$$

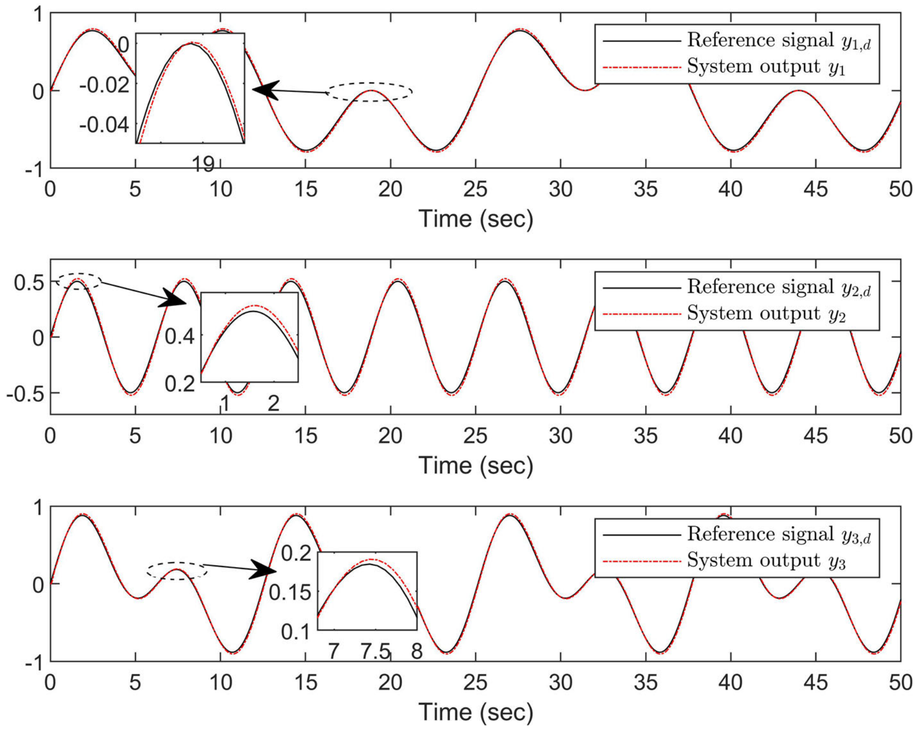

Fig. 9 System output y_i and reference signal $y_{i,d}$ of Example 2

It follows from (42), we have

$$\begin{aligned}\dot{V} \le & -\sum_{i=1}^{N}\sum_{j=1}^{n_i}\left(r_{i,j}-b_M\right)z_{i,j}^2-\sum_{i=1}^{N}\upsilon_{i,1}^2\left(z_{i,1}^2\right)z_{i,1}^2+\frac{1}{2}\sum_{i=1}^{N}\sum_{j=1}^{n_i}\sum_{l=1}^{N}y_l^2\tilde{h}_{i,j,l}^2(y_l)\\ & +\frac{1}{2}\sum_{i=1}^{N}\sum_{j=1}^{n_i}\varsigma_{i,j}^2+\sum_{i=1}^{N}\sum_{j=1}^{n_i}\varepsilon_{i,j}+2\sum_{i=1}^{N}\sum_{j=1}^{n_i}j\delta_{i,j}+\sum_{i=1}^{N}\sum_{j=1}^{n_i}d_{i,j}(t)+\sum_{i=1}^{N}\frac{1}{\lambda_{i,0}}d_{i,0}\\ & -\sum_{i=1}^{N}\frac{1}{\lambda_{i,0}}\bar{c}_i r_i+\sum_{i=1}^{N}\sum_{j=1}^{n_i}\tilde{\boldsymbol{\theta}}_{i,j}^{\mathrm{T}}\left(z_{i,j}S_{m_{i,j}}-\Gamma_{i,j}^{-1}\dot{\hat{\boldsymbol{\theta}}}_{i,j}\right). \end{aligned} \tag{46}$$

According to (44), term $\sum_{i=1}^{N}\sum_{j=1}^{n_i}\tilde{\boldsymbol{\theta}}_{i,j}^{\mathrm{T}}\left(z_{i,j}S_{m_{i,j}}-\Gamma_{i,j}^{-1}\dot{\hat{\boldsymbol{\theta}}}_{i,j}\right)$ can be rewritten as

$$\begin{aligned}&\sum_{i=1}^{N}\sum_{j=1}^{n_i}\tilde{\boldsymbol{\theta}}_{i,j}^{\mathrm{T}}\left(z_{i,j}S_{m_{i,j}}-\Gamma_{i,j}^{-1}\dot{\hat{\boldsymbol{\theta}}}_{i,j}\right)\\ &\quad\le\frac{1}{2}\sum_{i=1}^{N}\sum_{j=1}^{n_i}\eta_{i,j}\left(\left\|\boldsymbol{\theta}_{i,j}\right\|^2-\tilde{\boldsymbol{\theta}}_{i,j}^{\mathrm{T}}\tilde{\boldsymbol{\theta}}_{i,j}\right)\end{aligned}$$

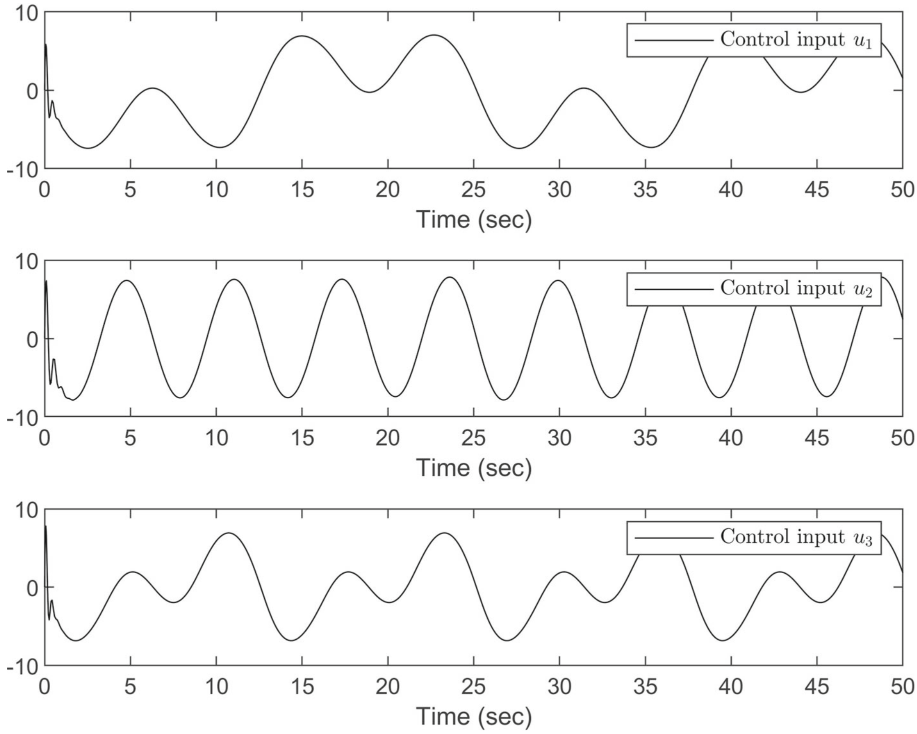

Fig. 10 Control inputs u_i of Example 2

$$\leq -\sum_{i=1}^{N}\sum_{j=1}^{n_i}\frac{1}{2\lambda_{\max}\left(\Gamma_{i,j}^{-1}\right)}\eta_{i,j}\tilde{\boldsymbol{\theta}}_{i,j}^{\mathrm{T}}\Gamma_{i,j}^{-1}\tilde{\boldsymbol{\theta}}_{i,j}+\frac{1}{2}\sum_{i=1}^{N}\sum_{j=1}^{n_i}\eta_{i,j}\left\|\boldsymbol{\theta}_{i,j}\right\|^2, \tag{47}$$

where $\lambda_{\max}\left(\Gamma_{i,j}^{-1}\right)$ represents the maximal eigenvalue of matrix $\Gamma_{i,j}^{-1}$.

The smooth and nonnegative function $\upsilon_{i,1}^2(\cdot)$ can be selected as

$$-\sum_{i=1}^{N}\upsilon_{i,1}^2\left(z_{i,1}^2\right)z_{i,1}^2+\frac{1}{2}\sum_{i=1}^{N}\sum_{j=1}^{n_i}\sum_{l=1}^{N}y_l^2\tilde{h}_{i,j,l}^2(y_l)\leq 0. \tag{48}$$

Combining (46), (47) and (48), the following inequality can be obtained

$$\begin{aligned}\dot{V}\leq&-\sum_{i=1}^{N}\sum_{j=1}^{n_i}\left(r_{i,j}-b_M\right)z_{i,j}^2-\sum_{i=1}^{N}\sum_{j=1}^{n_i}\frac{1}{2\lambda_{\max}\left(\Gamma_{i,j}^{-1}\right)}\eta_{i,j}\tilde{\boldsymbol{\theta}}_{i,j}^{\mathrm{T}}\Gamma_{i,j}^{-1}\tilde{\boldsymbol{\theta}}_{i,j}\\&+\frac{1}{2}\sum_{i=1}^{N}\sum_{j=1}^{n_i}\eta_{i,j}\left\|\boldsymbol{\theta}_{i,j}\right\|^2+\sum_{i=1}^{N}\sum_{j=1}^{n_i}d_{i,j}(t)+\frac{1}{2}\sum_{i=1}^{N}\sum_{j=1}^{n_i}\varsigma_{i,j}^2+\sum_{i=1}^{N}\sum_{j=1}^{n_i}\varepsilon_{i,j}\\&+2\sum_{i=1}^{N}\sum_{j=1}^{n_i}j\delta_{i,j}+\sum_{i=1}^{N}\frac{1}{\lambda_{i,0}}d_{i,0}-\sum_{i=1}^{N}\frac{1}{\lambda_{i,0}}\bar{c}_i r_i\end{aligned}$$

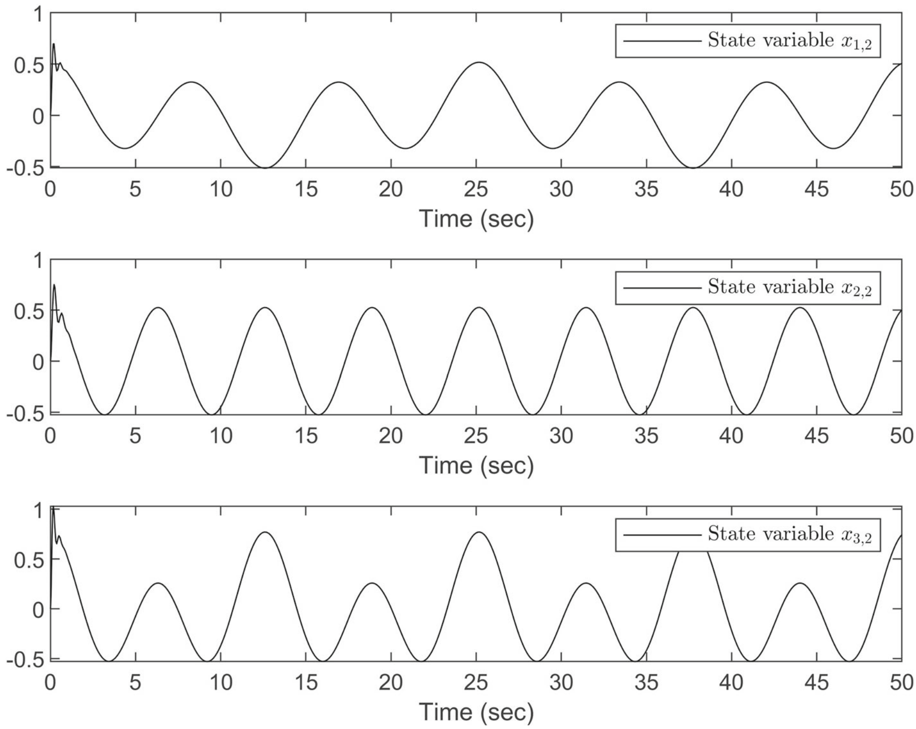

Fig. 11 State variables $x_{i,2}$ of Example 2

$$\leq -a_0 V + b_0 + \sum_{i=1}^{N} \sum_{j=1}^{n_i} d_{i,j}(t), \tag{49}$$

with $i = 1, 2, \ldots, N$, $j = 1, 2, \ldots, n_i$, $a_0 = \min\left\{2\left(r_{i,j} - b_M\right), \frac{\eta_{i,j}}{\lambda_{\max}\left(\Gamma_{i,j}^{-1}\right)}, \overline{c}_i\right\}$ and $b_0 = \frac{1}{2}\sum_{i=1}^{N}\sum_{j=1}^{n} \eta_{i,j} \left\|\boldsymbol{\theta}_{i,j}\right\|^2 + \frac{1}{2}\sum_{i=1}^{N}\sum_{j=1}^{n_i} \varsigma_{i,j}^2 + \sum_{i=1}^{N}\sum_{j=1}^{n_i} \varepsilon_{i,j} + 2\sum_{i=1}^{N}\sum_{j=1}^{n_i} j\delta_{i,j} + \sum_{i=1}^{N} \frac{1}{\lambda_{i,0}} d_{i,0}$.

For all $t \geq 0$, $\sum_{i=1}^{N}\sum_{j=1}^{n_i} d_{i,j}(t)$ is nonnegative. For all $t \geq T_{i,0}$, $\sum_{i=1}^{N}\sum_{j=1}^{n_i} d_{i,j}(t)$ is equal to zero. Therefore, the following inequality holds

$$\int_0^{\infty} \sum_{i=1}^{N} \sum_{j=1}^{n_i} d_{i,j}(t)dt < +\infty. \tag{50}$$

According to (50), the following inequality can be obtained

$$0 \leq V(t) \leq \left(V(0) - \frac{b_0}{a_0}\right)e^{-a_0 t} + \frac{b_0}{a_0} + \int_0^{\infty} \sum_{i=1}^{N} \sum_{j=1}^{n_i} d_{i,j}(t)dt, \ \forall t \geq 0. \tag{51}$$

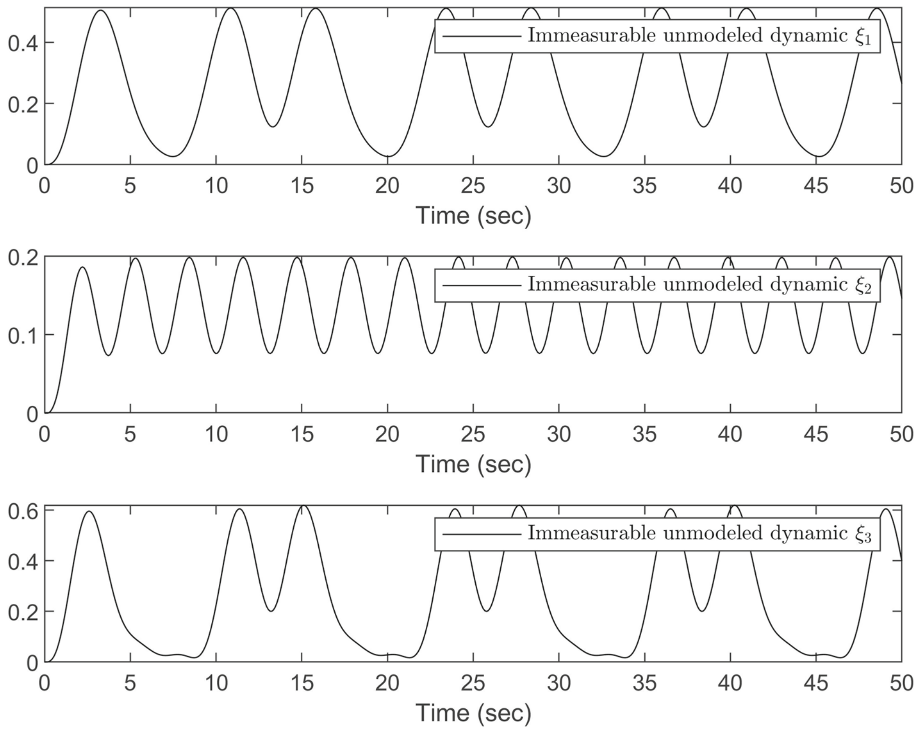

Fig. 12 Immeasurable unmodeled dynamics ξ_i of Example 2

Using the similar discussion in [30], it follows that all signals in the closed-loop systems are semi-globally bounded and the tracking error can converge to an adjustable neighborhood of the origin.

Based on the above analysis, it can be concluded that with the help of adaptive control laws, an adaptive MTN-based decentralized controller is designed for each subsystem. Therefore, the control process in this paper can be described as Fig. 2.

4 Simulation Results

In this section, a numerical example, a practical example and a comparative example are given to demonstrate the effectiveness of the proposed control strategy.

Example 1 Considering the following large-scale nonlinear systems with dynamic uncertainties

$$\begin{cases} \dot{\xi}_i = q_i \\ \dot{x}_{i,1} = g_{i,1}x_{i,2} + f_{i,1} + h_{i,1} + \Delta_{i,1} \\ \dot{x}_{i,2} = g_{i,2}u_i + f_{i,2} + h_{i,2} + \Delta_{i,2} \\ y_i = x_{i,1} \end{cases}, \tag{52}$$

where $i = 1, 2, 3$, $x_{i,1}(0) = x_{i,2}(0) = 0$, and $[\xi_1(0), \xi_2(0), \xi_3(0)]^{\mathrm{T}} = [0, 0, 0]^{\mathrm{T}}$, $q_1 = -\xi_1 + 0.5x_{1,1}^2 + x_{1,1}$, $g_{1,1} = 2 + 0.5\cos x_{1,1}^2$, $f_{1,1} = x_{1,1}^2$, $h_{1,1} = y_2 \cos y_1$, $\Delta_{1,1} = \xi_1 x_{1,1} \sin x_{1,1}$,

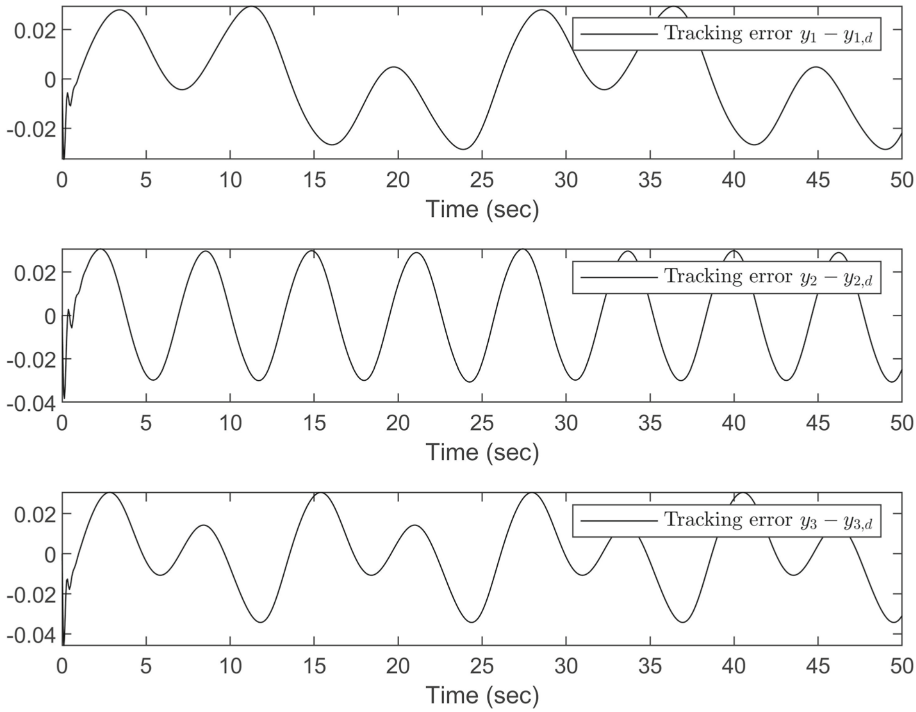

Fig. 13 Tracking error $y_i - y_{i,d}$ of Example 2

$g_{1,2} = 1 + \frac{x_{1,2}^2}{x_{1,1}^2 + x_{1,2}^2}$, $f_{1,2} = x_{1,2}^2 e^{-0.5x_{1,1}}$, $h_{1,2} = y_1 y_3$, $\Delta_{1,2} = \xi_1 x_{1,1} x_{1,2}$. $q_2 = -2\xi_2 + 0.5x_{2,1}^2 + 0.5$, $g_{2,1} = 2 + \sin x_{2,1}^2$, $f_{2,1} = x_{2,1}^2$, $h_{2,1} = y_3 \sin y_2$, $\Delta_{2,1} = \xi_2 x_{2,1} \sin x_{2,1}$, $g_{2,2} = 1 + \frac{x_{2,2}^2}{1 + x_{2,2}^2}$, $f_{2,2} = x_{2,2}^2 e^{-0.5x_{2,1}}$, $h_{2,2} = y_1 y_2^2$, $\Delta_{2,2} = \xi_2 x_{2,1} \sin x_{2,2}$, $q_3 = -3\xi_3 + 0.5x_{3,1}^2 + 1$, $g_{3,1} = 3 + 0.5 \sin x_{3,1}^2$, $f_{3,1} = x_{3,1}^2$, $h_{3,1} = y_1 \sin y_3$, $\Delta_{3,1} = \xi_3 x_{3,1} \sin x_{3,1}$, $g_{3,2} = 1 + \frac{x_{3,2}^2}{1 + x_{3,2}^2}$, $f_{3,2} = x_{3,2}^2 e^{-0.5x_{3,1}}$, $h_{3,2} = y_1 y_2 y_3$, $\Delta_{3,2} = \xi_3 x_{3,1} x_{3,2}$. The reference signals are set to $y_{1,d} = 0.5(\cos 0.25t - \cos 0.5t)$, $y_{2,d} = 0.5(\cos 0.75t - \cos 0.25t)$, $y_{3,d} = 0.5 \sin t$.

According to Theorem 1, the control structures are designed as (40), (43) and (44). The design parameters are set to $b_m = 1$, $b_M = 3$, $r_{1,1} = r_{1,2} = r_{2,1} = r_{2,2} = r_{3,1} = r_{3,2} = 10$, $\eta_{1,1} = \eta_{1,2} = \eta_{2,1} = \eta_{2,2} = \eta_{3,1} = \eta_{3,2} = 1$ and $\Gamma_{1,1} = \Gamma_{2,1} = \Gamma_{3,1} = I_5$, $\Gamma_{1,2} = \Gamma_{2,2} = \Gamma_{3,2} = I_9$.

The simulation results are shown in Figs. 3, 4, 5, 6 and 7, respectively.

Figure 3 shows the system output y_i and the reference signal $y_{i,d}$. As can be seen from Fig. 3, good tracking performance can be achieved. Figures 4, 5 and 6 depict the trajectories of the control input u_i, the state variables $x_{i,2}$ and immeasurable unmodeled dynamics ξ_i. Figure 7 shows that the tracking error can converge to an adjustable neighborhood of the origin.

Example 2 In order to further test the effectiveness of the control strategy proposed in this paper, the tripled inverted pendulums with unmodeled dynamics is considered, which is shown in Fig. 8 [33].

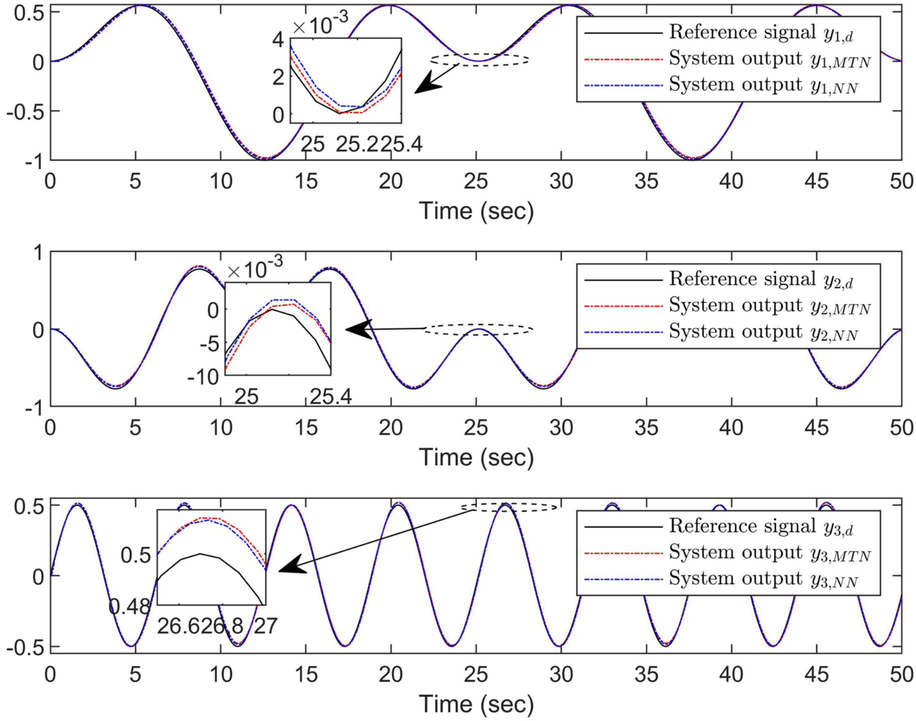

Fig. 14 The tracking performance comparison of MTN and RBFNN

where $\theta_i (i = 1, 2, 3)$ is the angle of the ith pendulum, l is the length of each rod, a is the distance from the pivot to the center of gravity of the rod, m_i is the mass of the ith rod, k_1 and k_2 are the spring constants and g is the gravitational acceleration.

Let $x_{i,1} = \theta_i$ and $x_{i,2} = \dot{\theta}_i$, the tripled inverted pendulum can be expressed as the following large-scale nonlinear systems with dynamic uncertainties.

$$\begin{cases} \dot{\xi}_i = q_i \\ \dot{x}_{i,1} = g_{i,1}x_{i,2} + f_{i,1} + h_{i,1} + \Delta_{i,1} \\ \dot{x}_{i,2} = g_{i,2}u_i + f_{i,2} + h_{i,2} + \Delta_{i,2} \\ y_i = x_{i,1} \end{cases}, \tag{53}$$

where $i = 1, 2, 3$, $j = 1, 2$, $x_{i,j}(0) = 0$, $\xi_i(0) = 0$, $q_1 = -\xi_1 + x_{1,1}^2$, $g_{1,1} = 1$, $f_{1,1} = h_{1,1} = \Delta_{1,1} = 0$, $g_{1,2} = 1$, $f_{1,2} = \frac{g}{l}\sin x_{1,1}$, $h_{1,2} = \frac{k_1a^2}{m_1l^2}(\sin y_2 \cos y_2 - \sin y_1 \cos y_1)$, $\Delta_{1,2} = \xi_1^2$, $q_2 = -\xi_2 + x_{2,1}^2$, $g_{2,1} = 1$, $f_{2,1} = h_{2,1} = \Delta_{2,1} = 0$, $g_{2,2} = 0.7$, $f_{2,2} = \frac{g}{l}\sin x_{2,1}$, $h_{2,2} = \frac{k_1a^2}{m_2l^2}(\sin y_1 \cos y_1 - \sin y_2 \cos y_2) + \frac{k_2a^2}{m_2l^2}(\sin y_3 \cos y_3 - \sin y_2 \cos y_2)$, $\Delta_{2,2} = \xi_2^2 \sin t$, $q_3 = -\xi_3 + x_{3,1}^2$, $g_{3,1} = 1$, $f_{3,1} = h_{3,1} = \Delta_{3,1} = 0$, $g_{3,2} = 1.2$, $f_{3,2} = \frac{g}{l}\sin x_{3,1}$, $h_{3,2} = \frac{k_2a^2}{m_3l^2}(\sin y_2 \cos y_2 - \sin y_3 \cos y_3)$, $\Delta_{3,2} = \xi_3^2 \cos t$. The given reference signals is considered as $y_{1,d} = 0.5(\sin 0.25t + \sin 0.75t)$, $y_{2,d} = 0.5 \sin t$, $y_{3,d} = 0.5(\sin t + \sin 0.5t)$. The parameters of systems (53) are designed as $g = 9.8$ m/s^2, $l = 1$ m, $a = 0.1$ m, $m_1 = m_2 = m_3 = 0.5$ Kg, $k_1 = 10$ N/m, $k_2 = 20$ N/m. The design parameters are chosen as: $b_m = 1$, $b_M = 1.2$, $\eta_{1,1} = \eta_{1,2} = \eta_{2,1} = \eta_{2,2} = \eta_{3,1} = \eta_{3,2} = 1$, $r_{1,1} = r_{2,1} = r_{3,1} = 30$, $r_{1,2} = r_{2,2} = r_{3,2} = 10$, $\Gamma_{1,1} = \Gamma_{2,1} = \Gamma_{3,1} = I_5$, $\Gamma_{1,2} = \Gamma_{2,2} = \Gamma_{3,2} = I_9$.

The simulation results are illustrated in Figs. 9, 10, 11, 12 and 13, respectively.

The simulation results further show that the control strategy proposed in this paper can achieve satisfactory results.

Remark 5 According to the definition of virtual control signal $\alpha_{i,j}$ and actual control input u_i, satisfactory tracking performance can be achieved when $r_{i,j}$, $\eta_{i,j}$ are positive constants and $\Gamma_{i,j}$ is a constant matrix. However, in practical applications, with the aim of achieving the superior tracking performance, it is necessary to select a set of optimal parameters through continuously adjusting the designed parameters.

Example 3 With the purpose of displaying the effectiveness of the proposed controller, based on Example 1, a comparative experiment is given. The comparison figure of tracking performance obtained by using MTN-based controller and radial basis function neural network (RBFNN)-based controller is shown below.

As can be seen from Fig. 14, similar tracking performance is achieved. It is worth noting that as a kind of NN with special structure, the middle layer of MTN uses polynomial rather than radial basis function. Therefore, from a structural point of view, the calculation speed of MTN control strategy is relatively fast.

5 Conclusion

The problem of adaptive tracking control for a class of large-scale nonlinear systems with unknown dynamic uncertainties is studied in this paper. The control process is designed based on backstepping and MTN technology. First of all, a dynamic signal is introduced to solve the unknown dynamic uncertainties problem effectively. Combining adaptive control with decentralized control, a MTN-based backstepping controller is proposed, which approximates unknown nonlinearity via MTN technology. The controller can ensure that all signals in the closed-loop systems are semi-global bounded, and the tracking error can converge to a small adjustable neighborhood of the origin. Finally, three simulation examples are given to verify the effectiveness of the proposed control strategy.

In the future work, a MTN-based adaptive fully distributed control method will be discussed for the problem considered in this paper. It is of great significance to provide an adaptive backstepping control strategy to balance dynamic uncertainties and random noise for large-scale nonlinear systems.

Funding Funding was provided by Natural Science Foundation of Shandong Province (Grant No. ZR2020QF055).

References

1. Zhou JH, Shi P, Gan DQ, Xu Y, Xin HH, Jiang CM, Xie H, Wu T (2017) Large-scale power system robust stability analysis based on value set approach. IEEE Trans Power Syst 32(5):4012–4023
2. Qu YC, Zhou XS (2017) Large-scale dynamic transportation network simulation: a space-time-event parallel computing approach. Transp Res Part C Emerg Technol 75:1–16

3. Goldschmid J, Corns S (2021) A cluster-based framework for interface analysis in large-scale aerospace systems. Syst Eng 24(5):339–351
4. Morariu C, Morariu O, Răileanu S, Borangiu T (2020) Machine learning for predictive scheduling and resource allocation in large scale manufacturing systems. Comput Ind 120:103244
5. Chen XF, Huang XY, Li J, Ma JF, Lou WJ, Wong DS (2015) New algorithms for secure outsourcing of large-scale systems of linear equations. IEEE Trans Inf Forensics Secur 10(1):69–78
6. Wang YS, Matni N, Doyle JC (2018) Separable and localized system-level synthesis for large-scale systems. IEEE Trans Autom Control 63(12):4234–4249
7. Liu Y, Liu XP, Jing YW, Wang HQ, Li XH (2021) Annular domain finite-time connective control for large-scale systems with expanding construction. IEEE Trans Syst Man Cybern Syst 51(10):6159–6169
8. Zhang X, Lin Y (2014) Nonlinear decentralized control of large-scale systems with strong interconnections. Automatica 50(9):2419–2423
9. Zhu Y, Fridman E (2020) Predictor methods for decentralized control of large-scale systems with input delays. Automatica 116:108903
10. Wang Z, Huang X, Shen H (2012) Control of an uncertain fractional order economic system via adaptive sliding mode. Neurocomputing 83:83–88
11. Wang W, Wen CY, Huang JS, Zhou J (2020) Adaptive consensus of uncertain nonlinear systems with event triggered communication and intermittent actuator faults. Automatica 111:108667
12. Wang W, Long J, Zhou J, Huang JS, Wen CY (2021) Adaptive backstepping based consensus tracking of uncertain nonlinear systems with event-triggered communication. Automatica 133:109841
13. Zhou J, Wen CY, Yang GH (2014) Adaptive backstepping stabilization of nonlinear uncertain systems with quantized input signal. IEEE Trans Autom Control 59(2):460–464
14. Jiang ZP (2000) Decentralized and adaptive nonlinear tracking of large-scale systems via output feedback. IEEE Trans Autom Control 45(11):2122–2128
15. Xie CH, Yang GH (2017) Decentralized adaptive fault-tolerant control for large-scale systems with external disturbances and actuator faults. Automatica 85:83–90
16. Du PH, Pan YN, Li HY, Lam HK (2021) Nonsingular finite-time event-triggered fuzzy control for large-scale nonlinear systems. IEEE Trans Fuzzy Syst 29(8):2088–2099
17. Wang HQ, Liu PXP, Bao JL, Xie XJ, Li S (2020) Adaptive neural output-feedback decentralized control for large-scale nonlinear systems with stochastic disturbances. IEEE Trans Neural Netw Learn Syst 31(3):972–983
18. Zhang J, Li S, Ahn CK, Xiang ZR (2022) Decentralized event-triggered adaptive fuzzy control for nonlinear switched large-scale systems with input delay via command-filtered backstepping. IEEE Trans Fuzzy Syst 30(6):2118–2123
19. Long LJ, Zhao J (2017) Decentralized adaptive neural output-feedback DSC for switched large-scale nonlinear systems. IEEE Trans Cybern 47(4):908–919
20. Tong SC, Sui S, Li YM (2014) Adaptive fuzzy decentralized output stabilization for stochastic nonlinear large-scale systems with unknown control directions. IEEE Trans Fuzzy Syst 22(5):1365–1372
21. Zhou Q, Shi P, Liu HH, Xu SY (2012) Neural-network-based decentralized adaptive output-feedback control for large-scale stochastic nonlinear systems. IEEE Trans Syst Man Cybern Part B Cybern 42(6):1608–1619
22. Han YQ, Li N, He WJ, Zhu SL (2021) Adaptive multi-dimensional Taylor network funnel control of a class of nonlinear systems with asymmetric input saturation. Int J Adapt Control Signal Process 35(5):713–726
23. Zhang JJ, Yan HS (2019) MTN optimal control of MIMO non-affine nonlinear time-varying discrete systems for tracking only by output feedback. J Franklin Inst 356(8):4304–4334
24. He WJ, Zhu SL, Li N, Han YQ (2022) Tracking control for switched nonlinear systems subject to output hysteresis via adaptive multi-dimensional Taylor network approach. Int J Control. https://doi.org/10.1080/00207179.2022.2067787
25. He WJ, Zhu SL, Li N, Han YQ (2022) Adaptive controller design for switched stochastic nonlinear systems subject to unknown dead-zone input via new type of network approach. Int J Control Autom Syst. **(Accepted)**
26. Han YQ (2021) Design of decentralized adaptive control approach for large-scale nonlinear systems subjected to input delays under prescribed performance. Nonlinear Dyn 106(1):565–582
27. Zhu SL, Han YQ (2022) Adaptive decentralized prescribed performance control for a class of large-scale nonlinear systems subject to nonsymmetric input saturations. Neural Comput Appl 34(13):11123–11140
28. Wang N, Lv SL, Er MJ, Chen WH (2016) Fast and accurate trajectory tracking control of an autonomous surface vehicle with unmodeled dynamics and disturbances. IEEE Trans Intell Veh 1(3):230–243
29. Zheng JZ, Yao JY (2019) Robust adaptive tracking control of hydraulic actuators with unmodeled dynamics. Trans Inst Meas Control 41(14):3887–3898

30. Jiang ZP, Praly L (1998) Design of robust adaptive controllers for nonlinear systems with dynamic uncertainties. Automatica 34(7):825–840
31. Cui D, Wu YF, Xiang ZR (2021) Finite-time adaptive fault-tolerant tracking control for nonlinear switched systems with dynamic uncertainties. Int J Robust Nonlinear Control 31(8):2976–2992
32. Feng SS, Sun ZY, Zhou CQ, Chen CC, Meng QH (2021) Output tracking control via neural networks for high-order stochastic nonlinear systems with dynamic uncertainties. Int J Fuzzy Syst 23:716–726
33. Liu YJ, Tong SC, Chen CLP (2013) Adaptive fuzzy control via observer design for uncertain nonlinear systems with unmodeled dynamics. IEEE Trans Fuzzy Syst 21(2):275–288
34. Tong SC, Liu CL, Li YM (2010) Fuzzy-adaptive decentralized output-feedback control for large-scale nonlinear systems with dynamical uncertainties. IEEE Trans Fuzzy Syst 18(5):845–861
35. Zhang TP, Xia XN (2015) Decentralized adaptive fuzzy output feedback control of stochastic nonlinear large-scale systems with dynamic uncertainties. Inf Sci 315:17–38
36. Zhang JJ (2021) Adaptive multi-dimensional Taylor network dynamic surface control for a class of strict-feedback uncertain nonlinear systems with unmodeled dynamics and output constraint. ISA Trans 108:35–47
37. Li YM, Tong SC (2015) Prescribed performance adaptive fuzzy output-feedback dynamic surface control for nonlinear large-scale systems with time delays. Inf Sci 292:125–142
38. Zhang J, Li S, Ahn CK, Xiang ZR (2021) Adaptive fuzzy decentralized dynamic surface control for switched large-scale nonlinear systems with full-state constraints. IEEE Trans Cybern. https://doi.org/10.1109/TCYB.2021.3069461
39. Han YQ (2018) Adaptive tracking control of nonlinear systems with dynamic uncertainties using neural network. Int J Syst Sci 49(7):1391–1402
40. Tong SC, Li YM, Shi P (2009) Fuzzy adaptive backstepping robust control for SISO nonlinear system with dynamic uncertainties. Inf Sci 179(9):1319–1332
41. He WJ, Han YQ, Li N, Zhu SL (2022) Novel adaptive controller design for a class of switched nonlinear systems subject to input delay using multi-dimensional Taylor network. Int J Adapt Control Signal Process 36(3):607–624